The use of post-production waste generated in the brewing industry for the effective bioremoval of Cu(II) ions

Tomasz Kalak

Department of Industrial Products and Packaging Quality, Institute of Quality Science, Poznań University of Economics and Business, Niepodległości 10, 61-875 Poznań, Poland, email: tomasz.kalak@ue.poznan.pl

ABSTRACT

In recent years, there has been significant industrial development in various parts of the world, which brings many benefits for society. Unfortunately, an increase in consumerism is also contributing to environmental degradation. Water contamination with toxic substances has become a serious global problem that requires solutions and immediate action. One of the most toxic pollutants are heavy metals, high concentration of which causes dysfunction and diseases of many organs in human body. A promising alternative among the various treatment methods is a biosorption process using cheap and readily available biosorbents. Noteworthy is post-production waste from the brewing industry in the form of brewer's grains, which have a strong affinity for binding metal ions and removing them from aqueous solutions due to the presence of appropriate organic functional groups in their composition. In this study, physicochemical properties and morphology of the brewer's spent grains were determined, and high efficiency of Cu(II) ions removal from aqueous solutions using biosorption processes was demonstrated. On the basis of the conducted research, the influence of various factors on the process efficiency and adsorption capacity was examined. Optimal conditions ensuring high biosorption efficiency were determined and process kinetics and adsorption isotherms were studied. The achieved results constitute a premise for the continuation of work on the potential use of brewery waste for the treatment of wastewater by retaining the heavy metals.

Keywords: Water quality; Brewing industry; Brewer's spent grains; Biosorption; Cu(II) ions

1. Introduction

The brewing industry is a dynamically developing sector of global economy and occupies a significant economic position. Technological development and scientific progress contribute to the production of more and more beer, increasing the assortment and improving quality of products. Beer is still the most popular alcoholic drink in the world, and among all beverages in general, it ranks fifth after tea, carbonated drinks, milk and coffee, excluding water [1–3]. According to the literature, beer was produced around several thousand years B.C. The production and consumption of beer favored the civilization development of society due to its important role in many traditional ceremonies, festivals and events. As shown in Fig. 1, global production increased from 1998 (1.3 bln hl (billion hectoliters)) to 2012 (1.96 bln hl) and has remained constant to this day at around 1.9–1.95 bln hl although in 2020 there was a decline in global production to around 1.82 bln hl, which was probably due to the COVID-19 pandemic. In 2020, China and the United States were the world's leading producers with the production of 341.11 mln hl (million hectoliters) and 211.17 mln hl, respectively [4]. In the European Union, Germany was the biggest manufacturer with the production of 7.5 billion
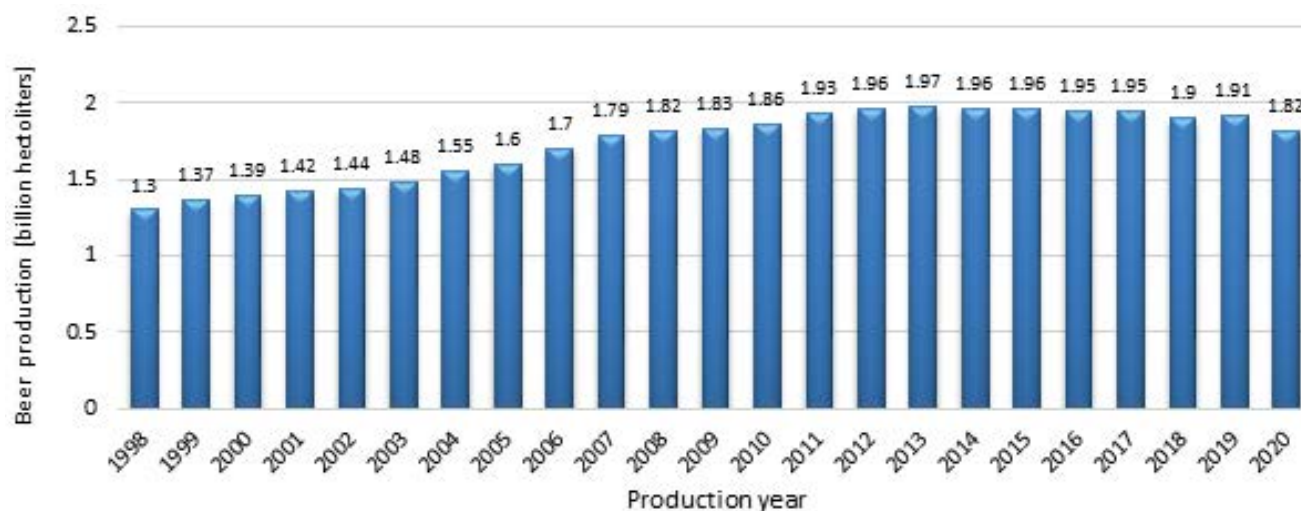
Fig. 1. Global beer production 1998–2020.

liters of beer (24%) in 2020. The next larger UE producers are as follows: Poland (3.8 bln L, 12%), Spain (3.3 bln L, 10%), the Netherlands (2.5 bln L, 8%), France (2.1 bln L, 7%), Czech Republic (1.8 bln L, 6%), Romania (1.7 bln L, 5%) and other countries (9.1 bln L, 28%) [5]. It is assumed that about 15–19 kg of a brewer's grains by-product (BG) with a dry matter content in the range of 35%–40% is generated by the production of about 100 hl of beer [8]. Based on these assumptions, it can be concluded that from about 27.3 to 34.58 million tons of post-production waste were generated in 2020 globally. Such amounts can be considered significant, creating many opportunities for their potential use for a variety of purposes, including the removal of metals from wastewater in sorption processes.

Large global production in the brewing industry generates an additional million tons of waste, which is an ecological, logistic and economic problem. As a result of production, large amounts of brewing valuable biomass is generated that can be used as animal feed, fuel, raw material in the production of methane and for many other purposes. This post-production material is rich in proteins, fats, amino acids, enzymes, fiber, polysaccharides, vitamins, flavor compounds, phytochemicals and minerals. These biomass components can also be recovered by extraction and then used as substrates in chemical, cosmetic, pharmacological and food production processes [6]. Another alternative, promising and pro-ecological solution may be the use of brewer's grains to purify wastewater from heavy metals and other toxic pollutants through biosorption processes. Our previous studies have proved that it is possible to bind metal ions by chemisorption and physicosorption due to the presence of many functional groups (e.g., amine, amide, carboxyl, phenol, etc.). The biosorption process is a technique that is characterized by low operating costs, mainly due to the use of cheap biowaste or by-products of the agri-food industry, easy availability of these materials, reduction of large amounts of waste. Particularly noteworthy is the high efficiency in removing metal ions from aqueous solutions. The costs of water treatment by

means of biosorption or adsorption are difficult to estimate as it depends on many factors, including the type of biomass used, parameters and the scale of the process. In the literature, several investigators provide information that the estimated costs can be in the range of about 5–200 USD/m³ and they are many times lower compared to the costs of other commercial methods of removing metal ions from wastewater, equal to about 10–450 USD/m³ [7,8].

The aim of this study was to use the post-production waste in the form of brewer's spent grains to determine efficiency of the biosorption process of Cu(II) ions in aqueous solutions. Additionally, the aim was also to determine the physicochemical properties of the biosorbent and to analyze kinetics of the processes and sorption isotherms.

2. Experimental procedure

2.1. Materials and methods

2.1.1. Preparation of research samples

In this study, samples of brewer's grains (BG) were obtained as a result of the process of obtaining beer in one of the Polish factories of the brewing industry (Fig. 2). The residues were wet biomass after being taken from the production process, therefore they were dried at 60°C to constant weight, and next cooled in a desiccator. Then the biomass was ground and screened through a sieve in order to select grains with a diameter ranging less than 0.212 mm. The samples prepared in this way were used in the experiments. All chemical compounds used in the study were pure for analysis. Deionized water was used in the research.

2.1.2. Characterisation of brewer's grains

Samples of brewer's grains (BG) with a diameter less than 0.212 mm were used in the research. Firstly, the biomass was examined for its physicochemical properties, including scanning electron microscopy-energy-dispersive X-ray spectroscopy (SEM-EDS) analysis, particle-size

Fig. 2. Brewer's spent grains used in the studies.

distribution, Brunauer–Emmett–Teller (BET) and Barrett–Joyner–Halenda (BJH), zeta potential, thermogravimetric analysis (TGA) and derivative thermogravimetry (DTG), SEM, Fourier-transform infrared spectroscopy (FT-IR). The methods were described in details and attached to the article as supplementary material (SM Methods).

2.1.3. Cu(II) sorption experiments

Biosorption efficiency of Cu(II) ions on brewer's grains (BG) was determined in batch experiments at room temperature (23°C). $CuCl_2$ (standard solution 1 g/L, Sigma-Aldrich) was used in the research. BG samples (2.5–100 g/L) and Cu(II) stock solution (portion volume V = 20 mL), and at initial pH 2–5 were shaken at 200 rpm in conical flasks for 60 min until equilibrium was reached. pH of Cu(II) stock solutions was adjusted with 0.1 M HCl and NaOH. In next stage, phases in the solutions were separated by a centrifugation process for 15 min (4,000 rpm). The concentration of copper(II) ions was determined using MP-AES plasma emission technique operating on microwave nitrogen plasma (Agilent 4210 MP-AES Apparatus, Agilent Technologies, Melbourne, Australia). Three repetitions of the measurements under normal pressure were used and the results were reported as mean values of all replicates. The biosorption efficiency (%) and the biosorption capacity (mg/g) were calculated in accordance with Eqs. (1) and (2):

$$R = \left[\frac{C_0 - C_e}{C_0}\right] \times 100\% \tag{1}$$

$$q_e = \frac{(C_0 - C_e) \times V}{m} \tag{2}$$

where C_0 is the initial concentration of Cu(II) ions (mg/L), C_e is the equilibrium concentration of Cu(II) ions (mg/L), V is the volume of solution (L), m is the mass of BG biosorbent (g).

Studies on sorption isotherms and kinetics were performed based on Langmuir and Freundlich models, pseudo-first-order and pseudo-second-order models, in accordance with the following Eqs. (3)–(6), respectively:

$$q_e = \frac{q_{max}K_L C_e}{1 + K_L C_e} \leftrightarrow \frac{C_e}{q_e} = \frac{1}{K_L q_{max}} + \frac{C_e}{q_{max}} \tag{3}$$

$$q_e = K_F C_e^{\frac{1}{n}} \leftrightarrow \ln q_e = \frac{1}{n}\ln C_e + \ln K_f \tag{4}$$

$$q_t = q_e\left(1 - e^{-k_1 t}\right) \leftrightarrow \log\left(q_e - q_t\right) = \log q_e - \frac{k_1}{2.303}t \tag{5}$$

$$q_t = \frac{q_e^2 k_2 t}{1 + q_e k_2 t} \leftrightarrow \frac{t}{q_t} = \frac{1}{q_e^2 k_2} + \frac{t}{q_e} \tag{6}$$

where q_{max} is the maximum biosorption capacity (mg/g); K_L is the Langmuir constant; C_e is the equilibrium concentration after the biosorption process (mg/L); K_F is the Freundlich constant; $1/n$ is the intensity of biosorption; q_t is the amount of Cu(II) ions (mg/g) adsorbed at any time t (min); q_e is the maximum amount of Cu(II) ions adsorbed per mass of BG at equilibrium (mg/g); k_1 is the rate constant of pseudo-first-order adsorption (1/min); k_2 is the rate constant of pseudo-second-order adsorption (g/(mg·min)).

3. Results and discussion

3.1. Characterization of the materials

The BG materials are classified as waste (code 02 07 80) and defined as decoctions, post-fermentation must sediments and bagasse, on the basis of the Regulation of the Polish Minister of Environment on waste [9,10]. The BG residues are characterised by a bread-like and grain-like aroma and a color of various shades of brown. The main ingredients are wheat, maize, barley malt, barley, rice and hops. The moisture content of the post-production biomass is estimated to be around 77%–82%. The most important nutrients are fats, carbohydrates, proteins, cellulose, hemicellulose, lignin, starch, crude ash, crude fibers, B vitamins, sodium, potassium, calcium, magnesium, phosphorus, methionine, lysine and others depending on the origin of the biomaterial components. According to average estimates, the total amount of nutrients is around 66% by dry matter, including approximately 26% protein and 14% sugar and starch [8]. Based on literature review, chemical composition of brewer's grains is presented in Table 1.

Bearing in mind the purpose of the BG post-production biomass specified in the Regulation of the Polish Minister of Environment (Journal of Laws of 2006, 06.49.356, Appendix 1), the residues can be used for feeding animals [25]. Among the benefits of feeding farm animals with brewing waste, the following can be mentioned, such as the health-promoting effect of nutrients on the condition of animals, lower costs of feeding animals compared to commercial feed, as well as the lack of costs related to waste storage and disposal. The BG can also be used for

Table 1
Chemical composition of brewer's grains based on literature review

Chemical composition (% of dry weight)								References
Cellulose	Hemicellulose	Lignin	Protein	Lipids	Ash	Phenolics	Starch	
	51	No data	23.4	9.4	4.1	–	–	[11]
25.4	21.8	11.9	24	10.6	2.4	–	–	[12]
	45	19.6	20.3	–	4.1	–	–	[13]
21.9	29.6	21.7	24.6	–	1.2	–	–	[14]
	60.64	9.19	24.39	6.18	2.48	–	–	[15]
25.3	41.9	16.9	–	–	4.6	–	–	[16]
21.73	19.27	19.4	24.69	–	4.18	–	–	[17]
16.8	28.4	27.8	15.2	–	4.6	–	–	[18]
26	22.2	–	22.1	–	1.1	–	–	[19]
12	40	18.5	14.2	13	3.3	2	2.7	[20]
40.2	–	56.74	6.41	2.5	2.27	–	0.28	[21]
31–33	–	20–22	15–17	6–8	–	1–1.5	10–12	[22]
–	22–29	13–17	20–24	–	–	–	2–8	[23]
	45.9	12.6	20.3	–	4.1	–	–	[24]

other purposes, such as raw material for processing into activated carbon, for the production of various animal feeds, for the production of edible mushrooms, as a raw material for anaerobic digestion, for hydrothermal carbonization, as raw fuel or as an additive to fossil fuels in power plants, as biomass for gasification processes in the production of methane in biogas plants, for processing into solid fuel (briquettes, pellets), etc. [26,27]. Another alternative and promising application may be the removal of heavy metals from wastewater in biosorption processes, which is the subject of this study.

First studies consisted in characterizing physicochemical properties of BG particles. Based on the analysis of particle-size distribution using the laser diffraction method, the presence of one peak was found with the particle-size equal to 68 nm (Fig. S1). The result of particle-size distribution analysis is often used as a parameter for particle performance in many industrial processes. Due to the fact that brewer's spent grains are a mixture of many different substances, it is possible that during the analysis, heavier particles fell to the bottom of the solution. In contrast, the lighter and smaller particles could dissolve faster in the solution and form a more stable suspension. Hence, only particles suspended in the solution could be measured. The results show the non-homogeneity of the BG particles. According to the literature, the larger surface area of the particles and the greater number of active sites on the biosorbent are related to the smaller particle-size of the biosorbent material, which translates into a greater efficiency of removing metal ions from aqueous solutions. Therefore, it seems reasonable to use biosorbent fractions with the smallest particle-size in the experiments [28–30].

The SEM-EDS method was used for elemental analysis and the results are shown in Table 2 and Fig. 3. In the tested BG material, the presence of such elements as C, O, Na, Mg, Al, Si, K, Ca, Ti, Fe and oxides of CO_2, Na_2O, MgO, Al_2O_3, SiO_2, K_2O, CaO, TiO_2, Fe_2O_3 were observed. It is worth noting that this research method consists in taking a point measurement on the surface of the sample. BG biomass is heterogeneous and consists of a mixture of many substances, hence, the content of elements and their amount may be slightly different in different points of the sample.

In order to determine the distribution of various elements on the BG biomass, the SEM-EDS mapping method with the use of a backscattered detector was used. The analysis made it possible to observe the distribution of individual elements (C, O, Si, P, Mg, Al, Ca, Na, S). It was found that the intensity is not the same and depends on the properties of the material and the type of the element (Fig. S2).

In the next stage of the research, BET analysis was performed, on the basis of which parameters such as pore diameter (4.39 nm), pore volume (0.0046 cm^3/g) and specific surface area (4.218 m^2/g) were determined (Figs. S3–S5). The BET adsorption isotherm is slightly convex towards the pressure axis, which makes it similar in shape to the type III isotherm. According to the literature, the convex shape of the isotherm in the direction of pressure axis informs about situation when, after the first single adsorption of particles, there is an interaction between them and the adsorbent, which creates a situation favorable for the adsorption of further metal ions. The isotherm can also inform about the so-called cooperative adsorption, which means that the particles previously adsorbed in the process may increase the sorption of other free particles present in the solution. However, the poor interaction at the interface and the low relative pressure can reduce the adsorption efficiency [31].

In the temperature range 30°C–600°C, a thermogravimetric study of the tested biomass was carried out (Fig. S6). In the initial stage, the first material weight loss of approx. 1.8% was observed in the temperature range of about 30°C–130°C, which may be the result of evaporation of water molecules from the sample. In the next step, a very intense weight loss of about 38% was reported in the temperature range of 200°C–380°C. This phenomenon

Table 2
Elemental composition of brewer's spent grains

Elements	C	O	Na	Mg	Al	Si	K	Ca	Ti	Fe
Content, weight (%)	7.01	51.29	1.78	5.34	7.16	14.85	0.35	9.16	0.65	2.41
Content, atomic (%)	11.28	61.95	1.49	4.24	5.13	10.22	0.17	4.42	0.26	0.83
Oxides	CO_2	–	Na_2O	MgO	Al_2O_3	SiO_2	K_2O	CaO	TiO_2	Fe_2O_3
Content in oxides (%)	25.68	–	2.4	8.85	13.53	31.77	0.42	12.82	1.09	3.44
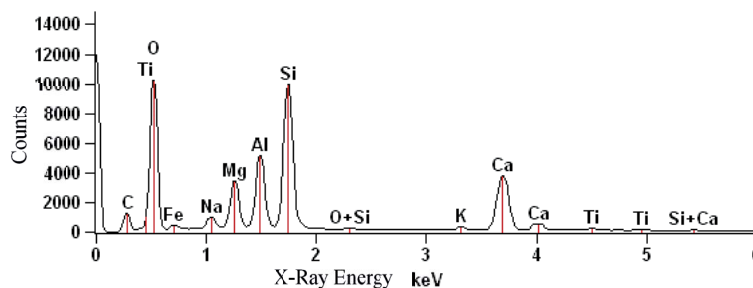
Fig. 3. EDS spectrum of brewer's spent grains.

could result from the pyrolysis process and gasification of volatile substances such as, for example, carbon dioxide. A very intense sharp peak (DTG) is visible at about 350°C–360°C, which can be attributed to the breakdown of proteins, carbohydrates or lipids. Other investigators have presented similar research results in the literature [32,33].

Subsequent studies concerned determination of electrokinetic zeta potential. This method allows to determine the effect of surface charge on biosorption of metal ions and to determine its efficiency [34]. In accordance with the literature, stability of suspension is greater when higher zeta potential values are observed, because electrostatically charged particles are repelled, thus eliminating their agglomeration and aggregation [35,36]. As a result of the analysis, it was found that the surface charge decreased almost in a straight line from –3 mV (pH 2) to –31 mV (pH 7) (Fig. S7). The isoelectric point (IEP) was not reached in this research and the electrostatic charge was only negative below the IEP point. At pH 2 it was revealed that $\zeta = -3.01$ which is close to the IEP. This means that IEP can probably be achieved in a very acidic solution in the pH range 0–2. In pH range 2.0–7.0, there were fewer negative particles on the surface of the BG biomaterial in relation to the positively charged particles. The isoelectric point (IEP) is zero at a specific pH of a solution, which is the equilibrium between positive and negative ions. Similar results have also been reported in the literature [37–39].

The SEM analysis was used to assess morphology of brewer's spent grains (Fig. 4). The images show particles of various sizes and shapes, including larger, elongated or smaller spherical ones. Both smaller and larger particles have irregular shapes. Fig. 4b shows a fibrous structure, which may indicate embryonic tissue or barley grain origin. Many of the particles are covered with small spherical projections, which are formations on the outer cells of seed coat. The visible spherical forms have a looser structure and are not densely set. Such irregular surface may contribute to particle chipping. Similar observations on the morphology of BG particles can be found in the literature [40–44].

FT-IR analysis of the BG samples before and after the biosorption process (at pH 4) with Cu(II) ions was carried out, and the spectra are presented in Fig. 5. Such features as band intensity, differences in shape, frequency and possible interactions of functional groups with Cu(II) metal ions were taken into account in the analysis. It was observed that the biosorption process shifted the intensity of bands towards lower transmittance as well as their position was slightly shifted or remained at the same wavelengths. The following changes can be highlighted: 3,284.83 (shift to 3,288.7 cm^{-1}), 2,923.72 (shift to 2,920.7 cm^{-1}), 1,643.84 (shift to 1,631.2 cm^{-1}), 1,515.88 (shift to 1,540.8 cm^{-1}), 1,225.6 (shift to 1,240.9 cm^{-1}), 1,032.92 (shift to 1,032.6 cm^{-1}). Band shifts may result from the interaction of functional groups of compounds present on the surface of BG material with Cu(II) ions, probably according to the mechanism of ion exchange (e.g., bonds formation between Cu^{2+} and nitrogen or oxygen atom). Ion exchange could take place between various metal cations (e.g., Na^+, K^+, Mg^{2+}, Fe^{3+}, Al^{3+}, Ca^{2+}) and Cu^{2+} ions. The presence of these metals in the BG sample was found as a result of the SEM-EDS analysis in this research (Table 2). On the surface of the biosorbent, ion exchange between ionizable cations or protons could occur.

Based on the analysis of the electrokinetic zeta potential, it was found that in the range of pH 2–7 there was a large predominance of negative charges on the surface of the BG biomass. This situation favors the presence of electrostatic attraction during the biosorption of Cu(II) ions in an aqueous solution. At pH 4, zeta potential ranged from about –16 to –17 mV, hence the greater number of electrons on the biomass surface attracted more Cu(II) ions in the solution, which translated into greater sorption capacity of the biosorbent [45].
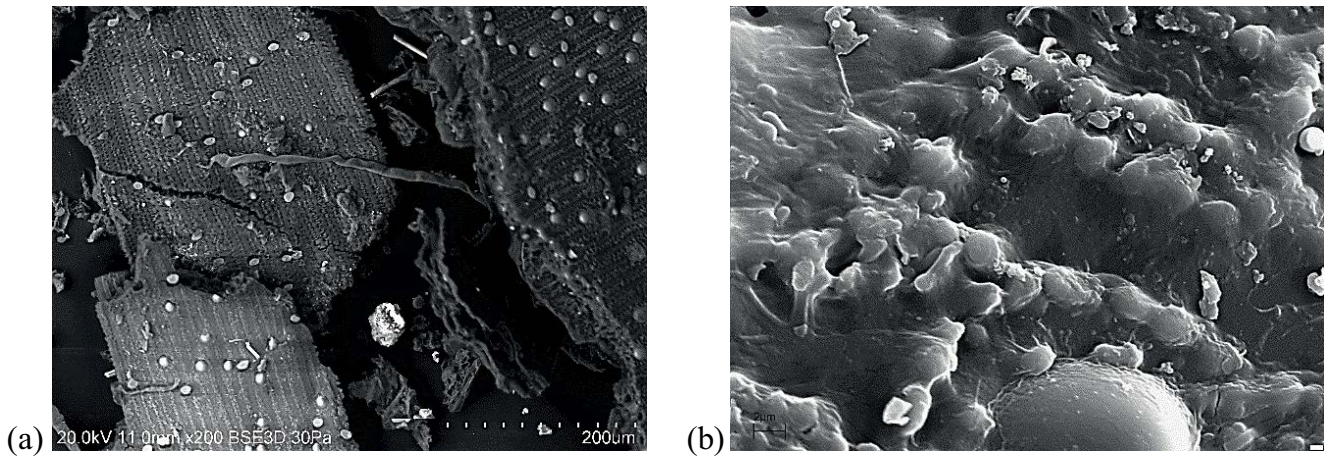
Fig. 4. SEM images of brewer's spent grains: (a) magn.: ×200, scale bar: 200 μm and (b) ×10,000, 2 μm.
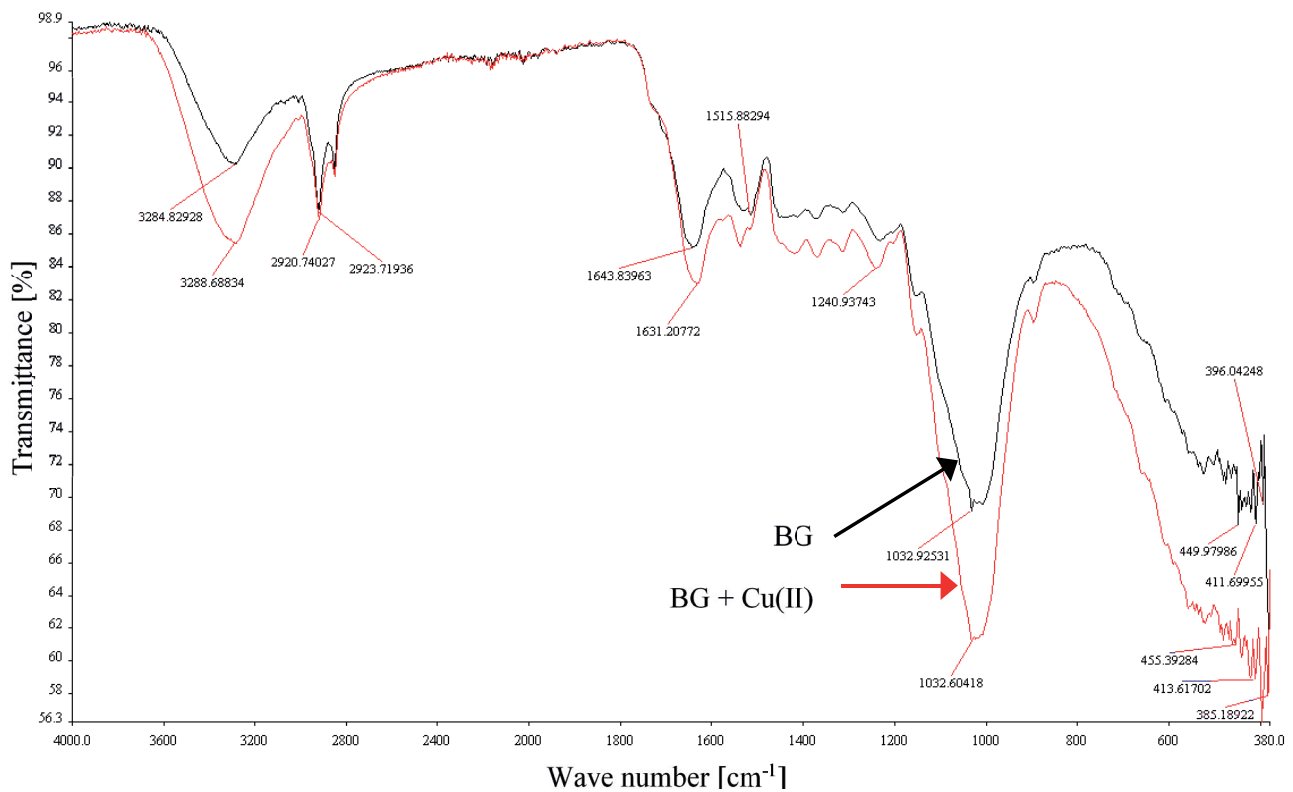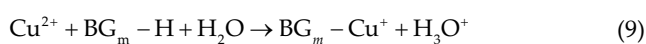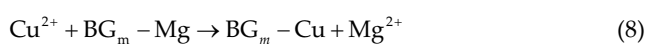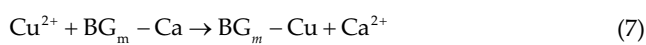

Fig. 5. FT-IR spectrum of brewer's spent grains before and after Cu(II) ions adsorption.

Considerations and interpretation of the research results suggest that sorption of Cu(II) ions could take place by ion exchange with exemplary Ca^{2+} and Mg^{2+} cations in accordance with general reactions (7–9):

$$Cu^{2+} + BG_m - Ca \rightarrow BG_m - Cu + Ca^{2+} \qquad (7)$$

$$Cu^{2+} + BG_m - Mg \rightarrow BG_m - Cu + Mg^{2+} \qquad (8)$$

$$Cu^{2+} + BG_m - H + H_2O \rightarrow BG_m - Cu^+ + H_3O^+ \qquad (9)$$

where: BG_m is the brewer's spent grain matrix.

3.2. Adsorption studies

3.2.1. Impact of initial pH

In the first phase of adsorption studies, the influence of initial pH on the process efficiency has been studied and the results are shown in Figs. 6 and S8. The research conditions were proposed as follows: initial concentration of Cu(II) ions 10.0 mg/L, BG dosage 2.5–100 g/L, initial pH range 2–5, rotational speed 200 rpm, T = 23°C,

contact time 60 min. The results clearly showed that the best biosorption efficiency was obtained at initial pH 4.0. Maximum biosorption has been reported for the following biosorbent doses: 7.98 g/L (R = 94.48%, initial pH 5), 70 g/L (R = 95.84%, initial pH 4). At initial pH 2 and 3, a gradual increase in sorption was noted up to pH 4, while a slight decrease at pH 5. Under conditions of initial pH 2, formation of copper chloride could take place, which in turn made it difficult to bind copper ions. In summary, it should be stated that the highest biosorption efficiency was demonstrated at the level of 94%–95.8%.

On the basis of the conducted research, it was found that binding of Cu^{2+} ions could take place based on the mechanism of ion exchange with other cations present on the surface of BG biosorbent. The surface of brewer's spent grains can be exposed to a large number of H^+ ions, which leads to an increase in the number of positively charged active centers, as well as a decrease in the number of negatively charged ones. Due to electrostatic repulsion, competition between H^+ and Cu^{2+} ions occurred in the aqueous solution, which contributed to interference with the sorption of positively charged Cu^{2+} ions. The surface of brewer's spent grains became more negatively electrostatically charged under the conditions of pH 3–4. In such a situation, acid groups were deprotonated, electrostatic affinity increased and ion exchange was initiated, which resulted in increased binding of more Cu^{2+} ions. In aqueous solutions copper exists in the ionic form in the range of pH 2–5, hence it can be bonded through various functional groups. This in turn precipitates as copper hydroxide when the pH of the solution is increased to alkaline

values. Thus, it was possible to obtain maximum sorption efficiency at pH 4. When the experiments were carried out at pH 5, sorption probably decreased as a result of competition of hydroxyl ions in the active sites. The factors slowing down and disturbing the sorption process include also formation of such forms as $Cu(OH)^+$ and $Cu(OH)_2$ [46,47].

3.2.2. Impact of BG sorbent dosage

Biosorption of Cu(II) ions onto brewer's spent grains was examined in terms of the influence of the adsorbent dose on the process efficiency (Fig. 7). The experimental
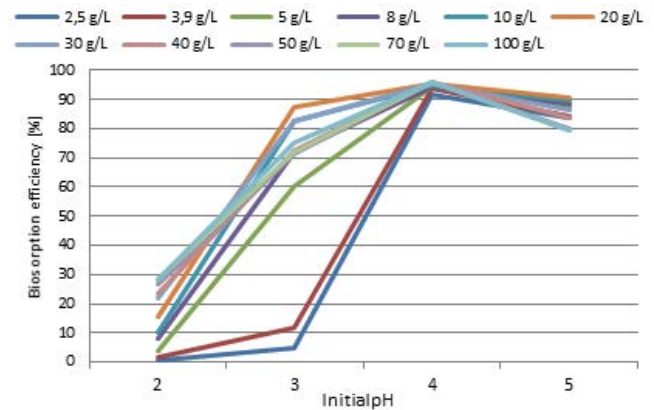

Fig. 6. Impact of initial pH on the Cu(II) biosorption efficiency (brewer's spent grains dosage 2.5–100 g/L).

Table 3
Parameters of pseudo-first-order and the pseudo-second-order models

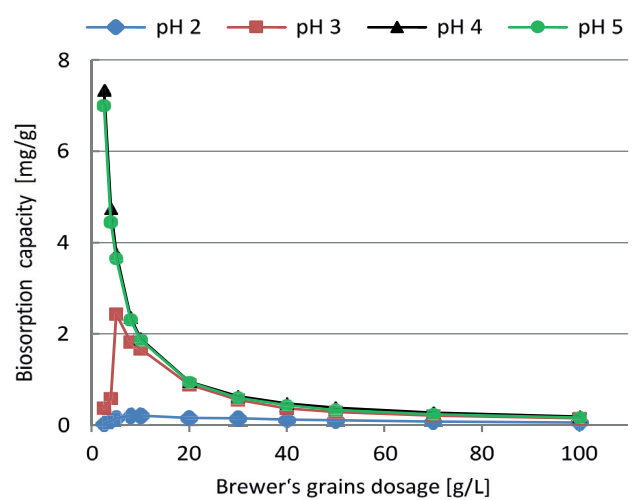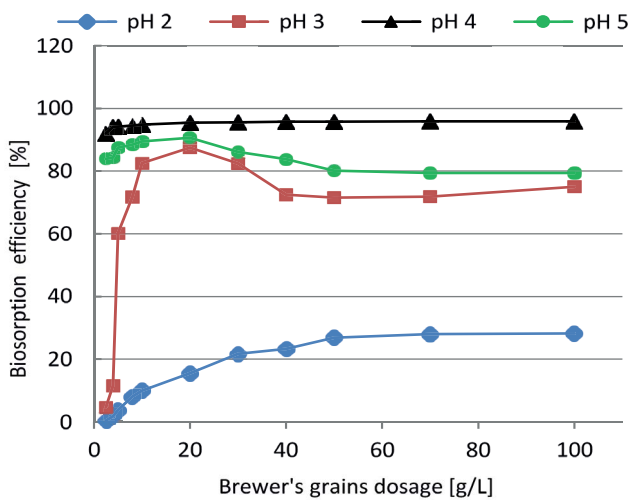| Metal ion	Adsorbent dosage (g/L)	Pseudo-first-order kinetic model			Pseudo-second-order kinetic model		
		k_{ad} (min^{-1})	q_e (mg/g)	R^2	k (g/mg min)	q_e (mg/g)	R^2
Cu(II)	10	0.03	0.087	0.887	1,173.77	0.064	0.986

Fig. 7. Impact of brewer's spent grains dosage on Cu(II) biosorption efficiency and biosorption capacity.

conditions were established as follows: initial concentration of Cu(II) ions 10.0 mg/L, initial pH 2–5, rotational speed 200 rpm, contact time 60 min, T = 23°C. After analyzing the research results, it was found that increasing BG dosage caused an increase in the efficiency of the Cu(II) ion removal process, which was also dependent on pH. Maximum sorption was observed at the dose of 10 g/L (pH 4) and in the range from 10 to 100 g/L the yield was about 95%–96%. In turn, the lowest biosorption was observed in aqueous solutions with an initial pH 2. Further increasing BG dose was not necessary due to the fact that no improvement in the efficiency of the process was noted. Additionally, it was found that biosorption capacity decreased from 7.3 mg/g (2.5 g/L, pH 4) to 0.06 mg/g (100 g/L, pH 2). At the lowest doses of BG sorbent (2.5 g/L), sorption capacity was higher. This means that saturation achieved, which may be a result of the availability of more sorption active sites, increased sorbent surface area, as well as completed particle interactions. The reduction of sorption capacity in the subsequent processes may be caused by aggregation or overlapping of active centers, which resulted in the reduction of the total sorbent surface. The obtained results suggest that both the sorbent dose and the concentration of adsorbed Cu(II) ions are indispensable for biosorption capacity [48].

3.2.3. Impact of initial concentration of Cu(II) ions

The influence of the initial concentration of Cu(II) ions on the biosorption efficiency has been investigated and the results are shown in Fig. 8. Previous results of the research gave indications to apply the following experimental conditions: initial concentration of Cu(II) ions (2.5–50 mg/L), adsorbent doses 2.5–25 g/L, initial pH 4, rotational speed 200 rpm, contact time 60 min, *T* = 23°C. Generally speaking, the increase in adsorption efficiency was noted in all cases. The best results (95.9%–96%) were observed with the brewer's grains dose of 10 g/L and a concentration range of 10–50 mg/L.

3.3. Adsorption kinetics

3.3.1. Impact of contact time

The influence of contact time on the biosorption process has been examined and the results are presented in Fig. 9. Based on my previous experiments, the following conditions for testing the influence of contact time have been established: initial concentration of Cu(II) ions 10 mg/L, initial pH 4.0, BG dosage 10 g/L, rotational speed 200 rpm, *T* = 23°C. The results clearly indicated that the highest sorption efficiency was recorded during the initial 5–10 min and this level (93%–96%) was maintained up to 8 h. It is estimated that under these experimental conditions the Cu(II) removal efficiency would remain unchanged after 1 h.

3.3.2. Studies of kinetic models

The biosorption of Cu(II) ions on brewer's spent grains was analyzed in terms of kinetics of the process. For this
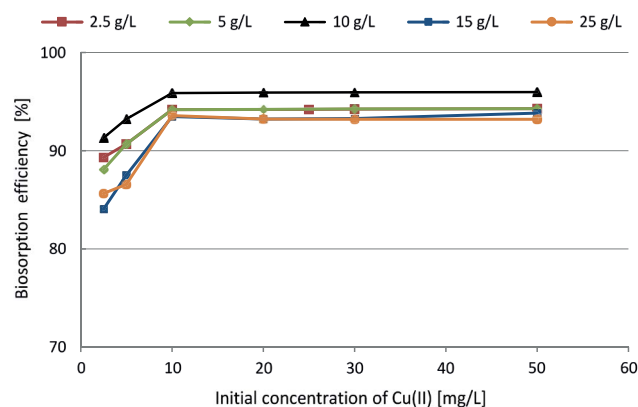

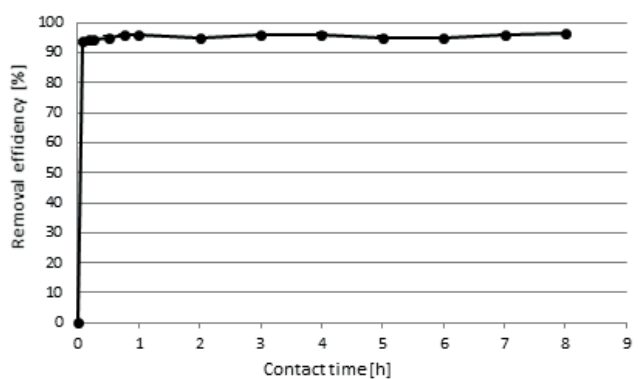Fig. 8. Impact of initial concentration of Cu(II) ions on biosorption efficiency.

Fig. 9. Effect of contact time on biosorption efficiency of Cu(II) ions.

purpose, pseudo-first-order and pseudo-second-order kinetic models were used to calculate the parameters of the sorption process, and the results are shown in Table 3 and Figs. S9 and S10. Equilibrium during the process was achieved after approx. 5–10 min. For the pseudo-first-order and pseudo-second-order reaction model, correlation coefficients are equal to $R^2 = 0.887$ and $R^2 = 0.986$, respectively. This suggests that the biosorption process is closer to the pseudo-second-order reaction model and may be based on ion exchange and electron sharing between copper ions and the sorbent surface [49]. In the process of biosorption, diffusion probably occurred and then ion exchange took place between the cations and Cu^{2+}. The active centers of BG surface could attract Cu^{2+} ions, which resulted in an increase in the number of coordination with the surface. The phenomenon of adhesion and formation of chemical bonds occurred on the surface of the biomass [50].

3.4. Analysis of isotherm models

Langmuir and Freundlich isotherms were used to analyze the Cu(II) biosorption process on BG waste and the calculated parameters are shown in Table 4 and Figs. S11–S20. By analyzing the results of the calculations, including the correlation coefficients, it can be concluded

Table 4
Parameters of Langmuir and Freundlich isotherms for biosorption of Cu(II) ions.

Metal ion	Biosorbent dosage (g/L)	Langmuir isotherm			Freundlich isotherm		
		Calculated q_m (mg/g)	K_L (L/mg)	R^2	K_F (mg/g) (L/mg)$^{(1/n)}$	n	R^2
Cu(II)	2.5	54.08	0.109	0.956	6.016	0.925	0.972
	5	59.96	0.046	0.960	2.995	0.911	0.974
	10	63.73	0.063	0.959	4.470	0.907	0.972
	15	66.98	0.011	0.935	0.819	0.871	0.951
	25	68.98	0.006	0.931	0.471	0.885	0.939

Table 5
Adsorption capacity of selected adsorbents for the removal of Cu(II) ions based on the literature

Adsorbents	q_{max} (mg/g)	References
Brewer's spent grains (BG)	68.98	These studies
Terminalia arjuna nuts coir pith	39.7	[54]
Mango peel	46.1	[55]
As-received ACF	9.0	[56]
Waste slurry	20.9	[57]
Penicillium chrysogenum	9.0	[58]
Chitosan/cotton fibers	24.8	[59]
Modified palm shell powder	45.3	[60]
Soybean straw	5.4	[61]
Activated poplar sawdust	9.2	[62]
Ammonium acetate modified sugarcane bagasse	35.5	[63]
Palm oil fruit shells	28–60	[64]
Groundnut shells	7.60	[65]
Guanyl-modified cellulose	83.0	[66]

that Cu(II) biosorption process is better inscribed in the Freundlich reaction model. Similar conclusions were also put forward by other researchers, for example, Allwar et al. [51], Stanković et al. [52], Adeoye et al. [53]. Additionally, the shape of the isotherms is determined by R_L parameter as follows: unfavorable ($R_L > 1$), linear ($R_L = 1$), favorable ($0 < R_L < 1$), irreversible ($R_L = 0$). In the present study, a favorable process for the removal of Cu(II) ions was found as the data was in the range $0 < R_L < 1$ [47]. In these studies, the highest biosorption efficiency is about 93%–96%, and the highest sorption capacity was obtained at the level of $q_m = 68.98$ mg/g, according to the calculations of the Langmuir equation. Table 5 shows a comparison of adsorption capacities of Cu(II) removal using various selected adsorbents published in the literature. As can be seen, q_{max} of brewer's spent grains is comparable or even greater than some adsorbents indicated by other researchers.

4. Conclusions

In this study, the process of biosorption of Cu(II) ions in aqueous solution using brewer's spent grains obtained during processing in the brewing industry was investigated. In the first stage, the biomass material was analyzed for physicochemical properties using various analytical techniques. Secondly, initial pH, BG sorbent dosage, contact time and initial concentration of Cu(II) were factors to be investigated for their effect on biosorption efficiency. It is particularly noteworthy that average efficiency of the processes under various experimental conditions was above 80%. Electrostatic attraction and ion exchange may be likely Cu(II) binding mechanisms. Thirdly, based on the analysis of process kinetics and adsorption isotherms it was showed that the pseudo-second-order kinetic model and Freundlich model better described the examined sorption processes. According to the Langmuir equation, calculated maximum biosorption capacity was equal to 68.98 mg/g.

To sum up, it should be assumed that the by-products of the brewing industry in the form of brewer's spent grains are capable of highly efficient removal of Cu(II) ions from aqueous solutions. This achievement is undoubtedly important and encourages further experiments in this area. The results of the research with the use of brewer's spent grains can potentially be used in the processes of metal removal from municipal and industrial wastewater as an alternative solution in line with the trend of circular economy.

Acknowledgements

Data availability statement

The data that support the findings of this study are available from the corresponding author upon reasonable request.

References

[1] J. Levinson, Malting-brewing: a changing sector, BIOS Int., 5 (2002) 12–15.
[2] S. Ciancia, Micro-brewing: a new challenge for beer, BIOS Int., 2 (2000) 4–10.
[3] M. de Oliveira Dias, Heineken brewing industry in Brazil, Int. J. Manage. Technol. Eng., 8 (2018) 1304–1310.
[4] J. Conway, Beer Production Worldwide From 1998 to 2019. Available at: https://www.statista.com/statistics/270275/worldwide-beer-production/ (Access: February 16, 2022).
[5] Products Eurostat News. Available at: https://ec.europa.eu/eurostat/web/products-eurostat-news/-/edn-20210805-1/ (Access: February 16, 2022).
[6] A.C. Fărcaș, S.A. Socaci, E. Mudura, F.V. Dulf, D.C. Vodnar, M. Tofană, L.C. Salanță, Exploitation of Brewing Industry Wastes to Produce Functional Ingredients, M. Kanauchi, Ed., Brewing Technology, InTechOpen, London, UK, 2017, pp. 137–156.
[7] V.K. Gupta, I. Ali, Environmental Water: Advances in Treatment, Remediation and Recycling, Elsevier, Amsterdam, The Netherlands, 2013, pp. 1–232.
[8] T. Kalak, J. Walczak, M. Ulewicz, Adsorptive recovery of Cd(II) ions with the use of post-production waste generated in the brewing industry, Energies, 14 (2021) 5543, doi: 10.3390/en14175543.
[9] The Act of 14 December 2012 on Waste (Polish Journal of Laws 2013, Item 21, As Amended).
[10] Regulation of the Minister of Environment of 11 May 2015 on Waste Recovery Outside of Installations and Devices (Polish Journal of Laws From 2015, Item 796).
[11] D. Yu, Y. Sun, W. Wang, S.F. O'Keefe, A.P. Neilson, H. Feng, Z. Wang, H. Huang, Recovery of protein hydrolysates from brewer's spent grain using enzyme and ultrasonication, Int. J. Food Sci. Technol., 55 (2020) 357–368.
[12] O. Kanauchi, K. Mitsuyama, Y. Araki, Development of a functional germinated barley foodstuff from brewer's spent grain for the treatment of ulcerative colitis, J. Am. Soc. Brew. Chem., 59 (2001) 59–62.
[13] K. Kemppainen, K. Rommi, U. Holopainen, K. Kruus, Steam explosion of brewer's spent grain improves enzymatic digestibility of carbohydrates and affects solubility and stability of proteins, Appl. Biochem. Biotechnol., 180 (2016) 94–108.
[14] F. Carvalheiro, M.P. Esteves, J.C. Parajó, H. Pereira, F.M. Gírio, Production of oligosaccharides by autohydrolysis of brewery's spent grain, Bioresour. Technol., 91 (2004) 93–100.
[15] O.P. Sobukola, J.M. Babajide, O. Ogunsade, Effect of brewers spent grain addition and extrusion parameters on some properties of extruded yam starch-based pasta, J. Food Process. Preserv., 37 (2013) 734–743.
[16] J.P. Silva, S. Sousa, J. Rodrigues, H. Antunes, J.J. Porter, I. Gonçalves, S. Ferreira-Dias, Adsorption of Acid orange 7 dye in aqueous solutions by spent brewery grains, Sep. Purif. Technol., 40 (2004) 309–315.
[17] N.G.T. Meneses, S. Martins, J.A. Teixeira, S.I. Mussatto, Influence of extraction solvents on the recovery of antioxidant phenolic compounds from brewer's spent grains, Sep. Purif. Technol., 108 (2013) 152–158.
[18] S.I. Mussatto, I.C. Roberto, Chemical characterization and liberation of pentose sugars from brewer's spent grain, J. Chem. Technol. Biotechnol., 81 (2006) 268–274.
[19] D.M. Waters, F. Jacob, J. Titze, E.K. Arendt, E. Zannini, Fibre, protein and mineral fortification of wheat bread through milled and fermented brewer's spent grain enrichment, Eur. Food Res. Technol., 235 (2012) 767–778.
[20] C. Xiros, E. Topakas, P. Katapodis, P. Christakopoulos, Hydrolysis and fermentation of brewer's spent grain by *Neurospora crassa*, Bioresour. Technol., 99 (2008) 5427–5435.
[21] K.M. Khidzir, A. Noorlidah, P. Agamuthu, Brewery spent grain: chemical characteristics and utilization as an enzyme substrate, Malays. J. Sci., 29 (2019) 41–51.
[22] A.J. Jay, M.L. Parker, R. Faulks, F. Husband, P. Wilde, A.C. Smith, C.B. Faulds, K.W. Waldron, A systematic micro-dissection of brewers' spent grain, J. Cereal Sci., 47 (2008) 357–364.
[23] J.A. Robertson, K.J.A. I'Anson, J. Treimo, C.B. Faulds, T.F. Brocklehurst, V.G.H. Eijsink, K.W. Waldron, Profiling brewers' spent grain for composition and microbial ecology at the site of production, LWT Food Sci. Technol., 43 (2010) 890–896.
[24] J. Treimo, B. Westereng, S.J. Horn, P. Forssell, J.A. Robertson, C.B. Faulds, K.W. Waldron, J. Buchert, V.G.H. Eijsink, Enzymatic solubilization of brewers' spent grain by combined action of carbohydrases and peptidases, J. Agric. Food Chem., 57 (2009) 3316–3324.
[25] Regulation of the Minister of Environment of 21 March 2006 on Waste Recovery Outside of Installations and Devices (Polish Journal of Laws 06.49.356, Appendix 1).
[26] W. Czekała, A. Pawlisiak, Produkcja i wykorzystanie wysłodzin browarnianych, Technika Rolnicza Ogrodnicza Leśna, 5 (2017) 23–25.
[27] M. Jackowski, Ł. Niedżwiecki, K. Jagiełło, O. Uchańska, A. Trusek, Brewer's spent grains—valuable beer industry by-product, Biomolecules, 10 (2020) 1669, doi: 10.3390/biom10121669.
[28] S.S. Alquzweeni, R.S. Alkizwini, Removal of cadmium from contaminated water using coated chicken bones with double-layer hydroxide (Mg/Fe-LDH), Water, 12 (2020) 2303, 1–13, doi: 10.3390/w12082303.
[29] Ch.Ch. Nnaji, S.Ch. Emefu, Effect of particle-size on the sorption of lead from water by different species of sawdust: equilibrium and kinetic study, Bioresources, 12 (2017) 4123–4145.
[30] Y. Tachibana, T. Kalak, M. Nogami, M. Tanaka, Combined use of tannic acid-type organic composite adsorbents and ozone for simultaneous removal of various kinds of radionuclides in river water, Water Res., 182 (2020) 116032, doi: 10.1016/j.watres.2020.116032.
[31] I.J. Alinnor, Adsorption of heavy metal ions from aqueous solution by fly ash, Fuel, 86 (2007) 853–857.
[32] A. Hejna, M. Barczewski, K. Skórczewska, J. Szulc, B. Chmielnicki, J. Korol, K. Formela, Sustainable upcycling of brewers' spent grain by thermo-mechanical treatment in twin-screw extruder, J. Cleaner Prod., 285 (2021) 124839, doi: 10.1016/j.jclepro.2020.124839.
[33] A.O. Balogun, F. Sotoudehnia, A.G Mcdonald, Thermo-kinetic, spectroscopic study of brewer's spent grains and characterisation of their pyrolysis products, J. Anal. Appl. Pyrolysis, 127 (2017) 8–16.
[34] M. Erdemoglu, M. Sarikaya, Effects of heavy metals and oxalate on the zeta potential of magnetite, J. Colloid Interface Sci., 300 (2006) 795–804.
[35] Ö. Demirbas, M. Alkan, M. Doğan, Y. Turhan, H. Namli, P. Turan, Electrokinetic and adsorption properties of sepiolite modified by 3-aminopropyltriethoxysilane, J. Hazard. Mater., 149 (2007) 650–656.
[36] T. Kalak, Y. Tachibana, Removal of lithium and uranium from seawater using fly ash and slag generated in the CFBC technology, RSC Adv., 11 (2021) 21964–21978.
[37] E.A. López-Maldonado, M.T. Oropeza-Guzmán, Strategic Design of Heavy Metals Removal Agents through Zeta Potential Measurements, H. El-Din M. Saleh, R.F. Aglan, Eds., Heavy Metals, InTechOpen, London, UK, 2018, pp. 53–65.
[38] M. Kosmulski, E. Mączka, The isoelectric point of an exotic oxide: tellurium(IV) oxide, Molecules, 26 (2021) 3136, doi: 10.3390/molecules26113136.

[39] A. Kołodziejczak-Radzimska, T. Jesionowski, Characterization of amino-, epoxy- and carbonyl-functionalized halloysite and its application in the immobilization of aminoacylase from *Aspergillus melleus*, Physicochem. Probl. Miner. Process., 55 (2019) 128–139.

[40] Y. Tao, Y. Han, W. Liu, L. Peng, Y. Wang, S. Kadam, P.L. Show, X. Ye, Parametric and phenomenological studies about ultrasound-enhanced biosorption of phenolics from fruit pomace extract by waste yeast, Ultrason. Sonochem., 52 (2019) 193–204.

[41] F.T.V. Rubio, G.M. Maciel, M.V. Silva, V.G. Correa, R.M. Peralta, C.W.I. Haminiuk, Enrichment of waste yeast with bioactive compounds from grape pomace as an innovative and emerging technology: kinetics, isotherms and bioaccessibility, Innovative Food Sci. Emerg. Technol., 45 (2018) 18–28.

[42] E. Ferraz, J. Coroado, J. Gamelas, J. Silva, F. Rocha, A. Velosa, Spent brewery grains for improvement of thermal insulation of ceramic bricks, J. Mater. Civ. Eng., 25 (2013) 1638–1646.

[43] A.A. Boateng, P.H. Cooke, K.B. Hicks, Microstructure development of chars derived from high-temperature pyrolysis of barley (*Hordeum vulgare* L.) hulls, Fuel, 86 (2007) 735–742.

[44] J. Olkku, E. Kotaviita, M. Salmenkallio-Marttila, H. Sweins, S. Home, Connection between structure and quality of barley husk, J. Am. Soc. Brew. Chem., 63 (2005) 17–22.

[45] J.-Y. Wang, Ch.-W. Cui, Characterization of the biosorption properties of dormant spores of *Aspergillus niger*: a potential breakthrough agent for removing Cu^{2+} from contaminated water, RSC Adv., 7 (2017) 14069–14077.

[46] C. Tu, Y. Liu, J. Wei, L. Li, K.G. Scheckel, Y. Luo, Characterization and mechanism of copper biosorption by a highly copper-resistant fungal strain isolated from copper-polluted acidic orchard soil, Environ. Sci. Pollut. Res. Int., 25 (2018) 24965–24974.

[47] J.B. Dulla, M.R. Tamana, S. Boddu, K. Pulipati, K. Srirama, Biosorption of copper(II) onto spent biomass of *Gelidiella acerosa* (brown marine algae): optimization and kinetic studies, Appl. Water Sci., 10 (2020) 56, doi: 10.1007/s13201-019-1125-3.

[48] T. Kalak, K. Marciszewicz, J. Piepiórka-Stepuk, Highly effective adsorption process of Ni(II) ions with the use of sewage sludge fly ash generated by circulating fluidized bed combustion (CFBC) technology, Materials, 14 (2021) 3106, doi: 10.3390/ma14113106.

[49] X.-H. Wang, R.-H. Song, S.-X. Teng, M.-M. Gao, J.-Y. Ni, F.-F. Liu, S.-G. Wang, B.-Y. Gao Characteristics and mechanisms of Cu(II) biosorption by disintegrated aerobic granules, J. Hazard. Mater., 179 (2010) 431–437.

[50] Y.S. Ho, J.C.Y. Ng, G. McKay, Kinetics of pollutant sorption by biosorbents: review, Sep. Purif. Rev., 29 (2000) 189–232.

[51] A. Allwar, A. Setiawan, H.A. Ermawan, T. Alviansah, Removal of Cu(II) ions from aqueous solution by activated carbon produced from banana fruit bunch (*Musa paradisiaca*), Desal. Water Treat., 172 (2019) 139–147.

[52] S. Stanković, T. Šoštarić, M. Bugarčić, A. Janićijević, K. Pantović-Spajić, Z. Lopičić, Adsorption of Cu(II) ions from synthetic solution by sunflower seed husks, Acta Period. Technol., 50 (2019) 268–277.

[53] B.K. Adeoye, B.A. Akinbode, J.D. Awe, C.T. Akpa, Evaluation of biosorptive capacity of waste watermelon seed for lead(II) removal from aqueous solution, Am. J. Environ. Eng., 10 (2020) 1–8.

[54] A. Lopez-Delgado, C. Perez, F.A. Lopez, Sorption of heavy metals on blast furnace sludge, Water Res., 32 (1998) 989–996.

[55] M. Iqbal, A. Saeed, I. Kalim, Characterization of adsorptive capacity and investigation of mechanism of Cu^{2+}, Ni^{2+} and Zn^{2+} adsorption on mango peel waste from constituted metal solution and genuine electroplating effluent, Sep. Sci. Technol., 44 (2009) 3770–3791.

[56] J.R. Rangel-Mendez, M. Streat, Adsorption of cadmium by activated carbon cloth: influence of surface oxidation and solution pH, Water Res., 36 (2002) 1244–1252.

[57] S.M. Lee, A.P. Davis, Removal of Cu(II) and Cd(II) from aqueous solution by seafood processing waste sludge, Water Res., 35 (2001) 534–540.

[58] S.S. Ahluwalia, D. Goyal, Microbial and plant derived biomass for removal of heavy metals from wastewater, Bioresour. Technol., 98 (2007) 2243–2257.

[59] W.S. Wan Ngah, L.C. Teong, M.A.K.M. Hanafiah, Adsorption of dyes and heavy metal ions by chitosan composites: a review, Carbohydr. Polym., 83 (2011) 1446–1456.

[60] S. Kushwaha, B. Sreedhar, R. Bhatt, P.P. Sudhakar, Spectroscopic characterization for remediation of copper, cadmium and mercury using modified palm shell powder, J. Taiwan Inst. Chem. Eng., 46 (2015) 191–199.

[61] M. Šćiban, M. Klašnja, B. Škrbić, Adsorption of copper ions from water by modified agricultural by-products, Desalination, 229 (2008) 170–180.

[62] F.N. Acar, Z. Eren, Removal of Cu(II) ions by activated poplar sawdust (Samsun Clone) from aqueous solutions, J. Hazard. Mater., 137 (2006) 909–914.

[63] G. Li, M. Wang, X. Chen, X. Li, Adsorption performance for the removal of Cu(II) on the ammonium acetate modified sugarcane bagasse, Nat. Environ. Pollut. Technol., 16 (2017) 843–848.

[64] M.A. Hossain, H.H. Ngo, W.S. Guo, T.V. Nguyen, Palm oil fruit shells as biosorbent for copper removal from water and wastewater: experiments and sorption models, Bioresour. Technol., 113 (2012) 97–101.

[65] S.R. Shukla, R.S. Pai, Adsorption of Cu(II), Ni(II) and Zn(II) on dye loaded groundnut shells and sawdust, Sep. Purif. Technol., 43 (2005) 1–8.

[66] I.M. Kenawy, M.A. Hafez, M.A. Ismail, M.A. Hashem, Adsorption of Cu(II), Cd(II), Hg(II), Pb(II) and Zn(II) from aqueous single metal solutions by guanyl-modified cellulose, Int. J. Biol. Macromol., 107 (2018) 1538–1549.

Supplementary information

S1. Methods of brewer's grains characterization

In the research, brewer's grains particles with a diameter less than 0.212 mm were used. Firstly, physical and chemical properties of the material were analyzed using several methods, including:

(1) Determination of particle-size distribution was performed by the laser diffraction method using a Zetasizer Nano ZS (Malvern Instruments Ltd., United Kingdom), which is capable of measuring powders with a size distribution ranging from 0.2 to 2,000 μm.

(2) The elemental composition and mapping of fly ash samples was examined with a scanning electron microscope (SEM) Hitachi S-3700N with an attached a Noran SIX energy-dispersive X-ray spectrometer (EDS) microanalyzer (ultra-dry silicon drift type with resolution (FWHM) 129 eV, accelerating voltage: 20.0 kV).
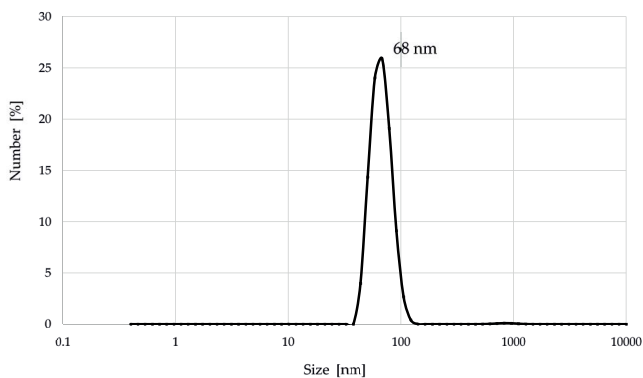

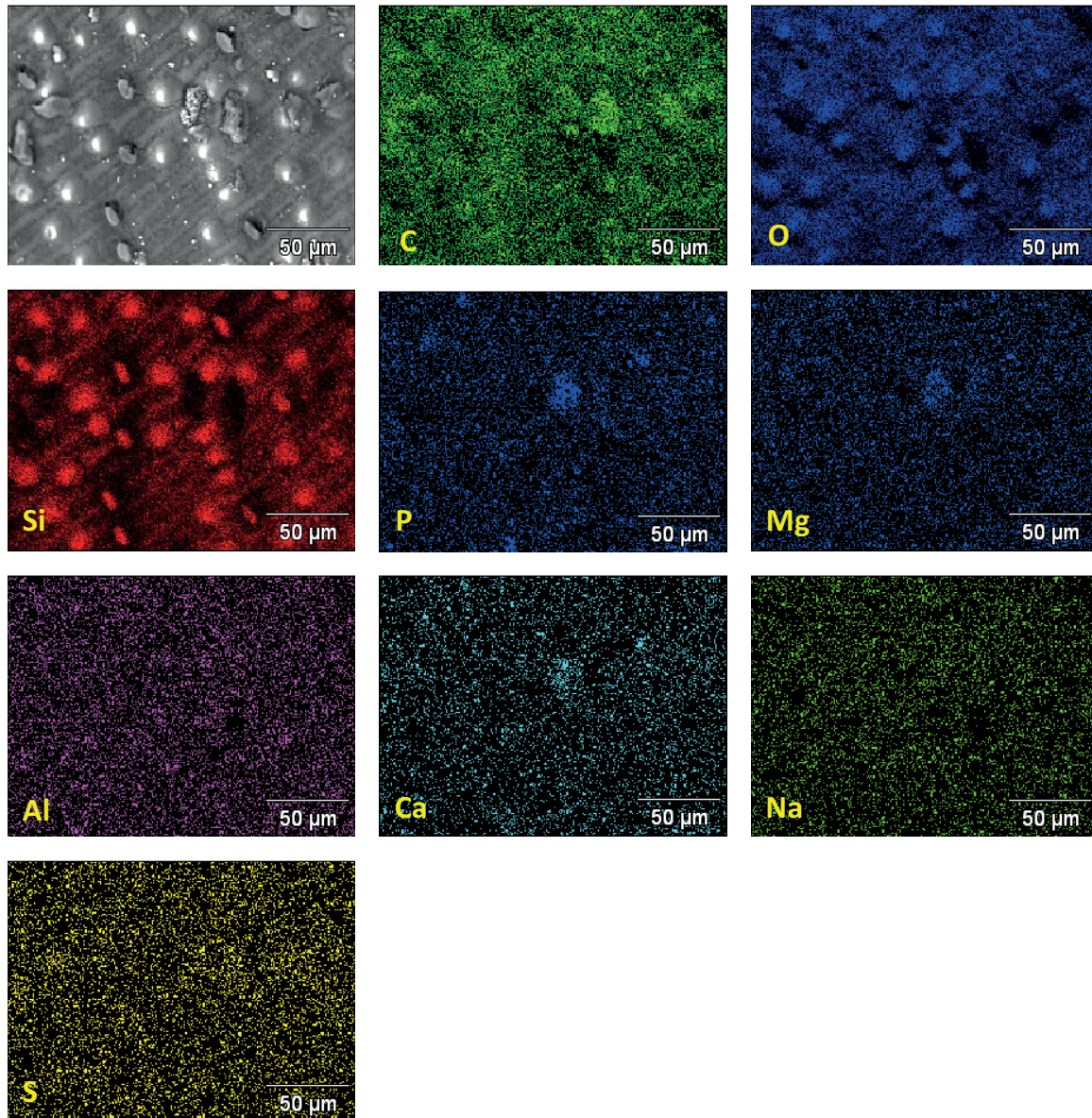Fig. S1. Particle-size distribution of brewer's grains.

Fig. S2. SEM-EDS images (mapping) of the distribution and relative proportion (intensity) of defined elements (C, O, Si, P, Mg, Al, Ca, Na, S) over the scanned area of brewer's spent grains (magn.: ×600, scale bar: 50 μm).

(3) Investigation of electrokinetic zeta potential was carried out using Zetasizer Nano ZS (Malvern Instruments Ltd., United Kingdom) equipped with autotitrator (MPT-2 Autotitrator). The apparatus uses a combination of electrophoresis and laser particle movement measurement based on the Doppler Effect. The instrument measures the rate of particle movement in the liquid after switching on the electric field. The speed of motion of the particle is defined as its electrophoretic mobility, which is automatically calculated and converted to the zeta potential using the Smoluchowski's Eq. (S1).

$$\zeta = \frac{4\pi\eta}{\mu}U \qquad (S1)$$

where: ζ is zeta potential; π is the constant; η is the viscosity of the suspending liquid; ε is the dielectric constant and U is the electrophoretic mobility. Ash samples were dispersed in distilled water and pH of the slurry was adjusted by addition 0.2 M HCl and 0.2 M KOH before measurements at room temperature (23°C ± 1°C) of electrophoretic mobility of particles.

(4) The specific surface area and the average pore diameter were determined with the Brunauer–Emmett–Teller (BET) method using Autosorb iQ Station 2 (Quantachrome Instruments, USA).

(5) The pore volume was determined by Barrett–Joyner–Halenda (BJH) method using Autosorb iQ Station 2 (Quantachrome Instruments, USA).
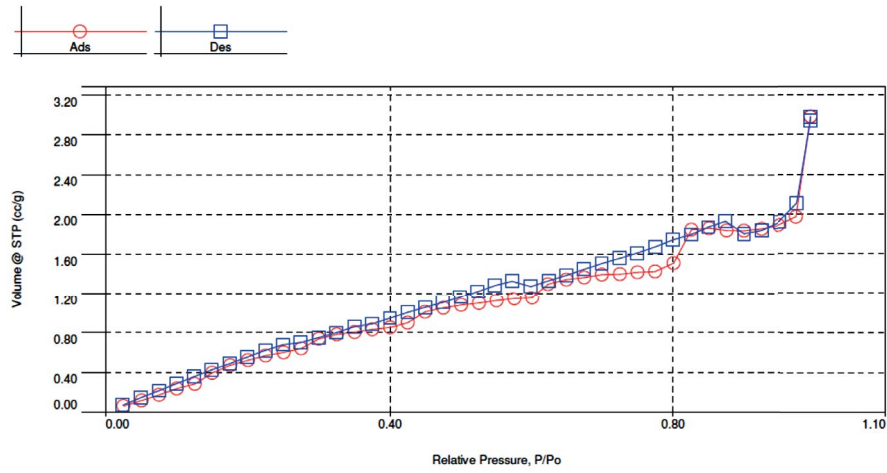
Fig. S3. Linear form of the BET adsorption and desorption isotherm of brewer's spent grains.
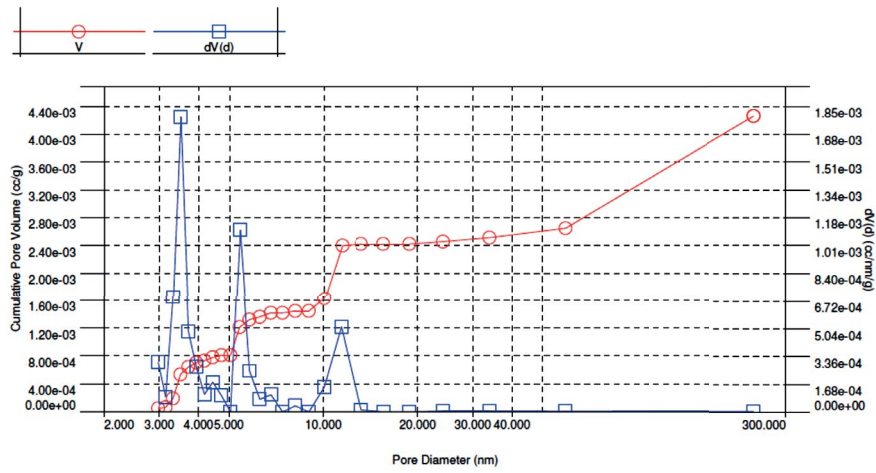
Fig. S4. Pore-size distribution in brewer's spent grains during adsorption.
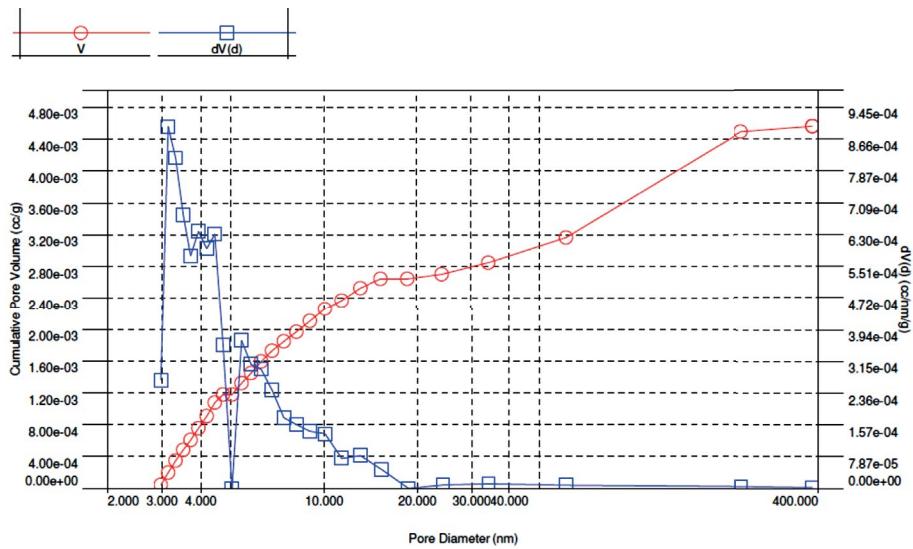
Fig. S5. Pore-size distribution in brewer's spent grains during desorption.
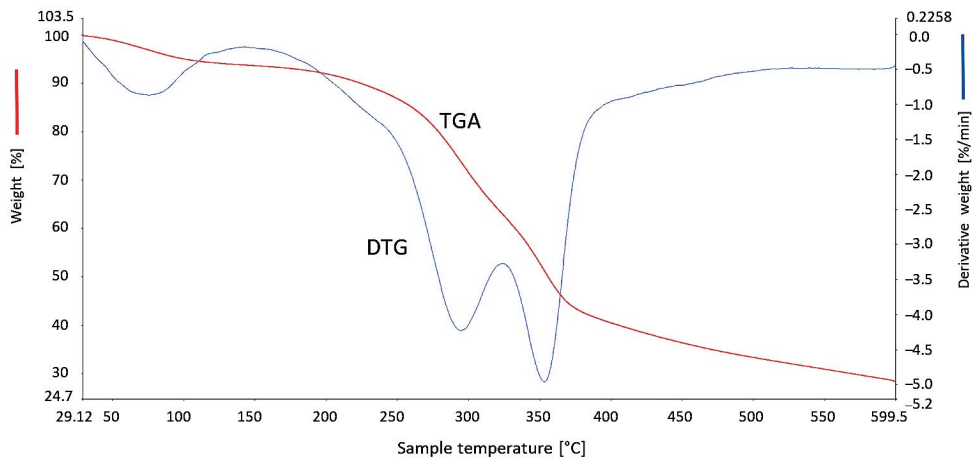
Fig. S6. Thermogravimetric curves of brewer's spent grains.
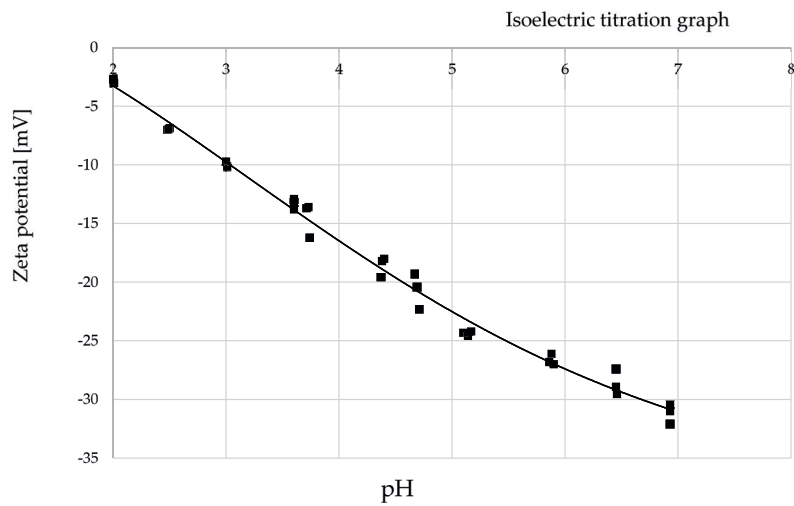
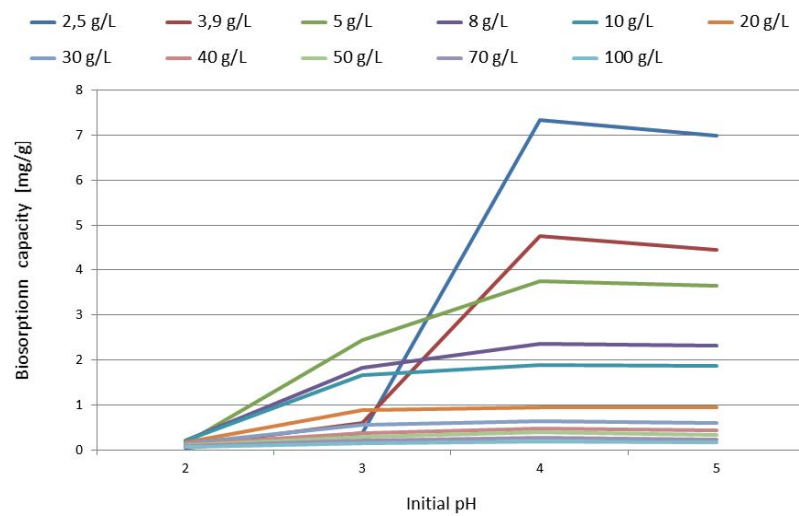Fig. S7. Change in zeta potential with equilibrium pH.

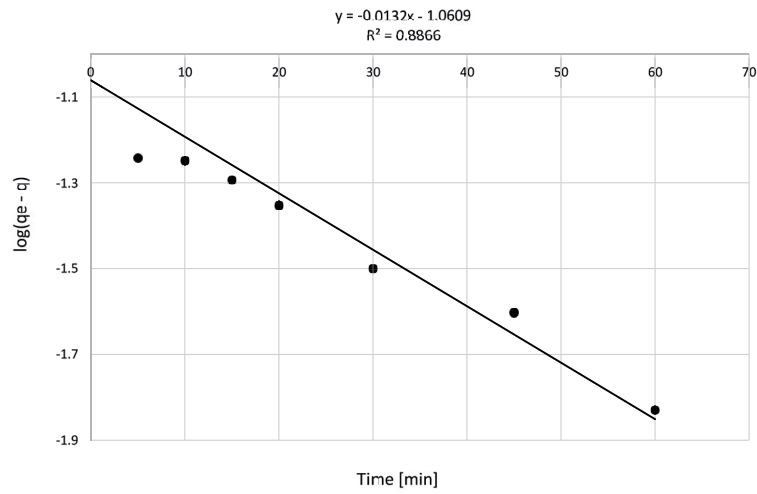Fig. S8. Impact of initial pH on the Cu(II) biosorption capacity (brewer's spent grains dosage 2.5–100 g/L).

Fig. S9. Pseudo-first-order isotherm for adsorption of Cu(II) ions on brewer's spent grains.
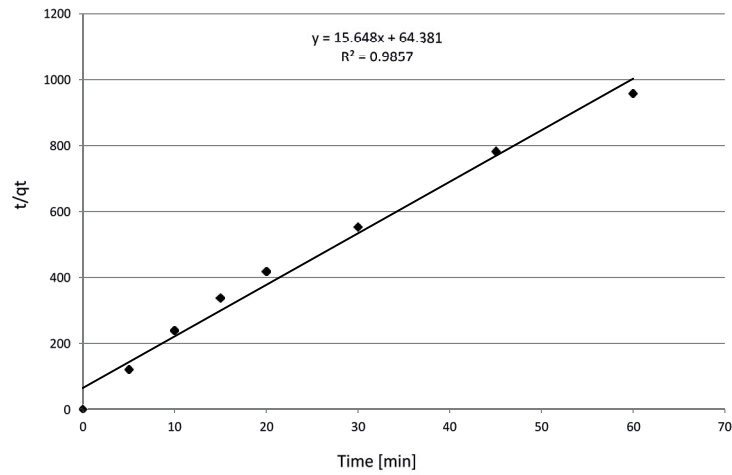
Fig. S10. Pseudo-second-order isotherm for adsorption of Cu(II) ions on brewer's spent grains.
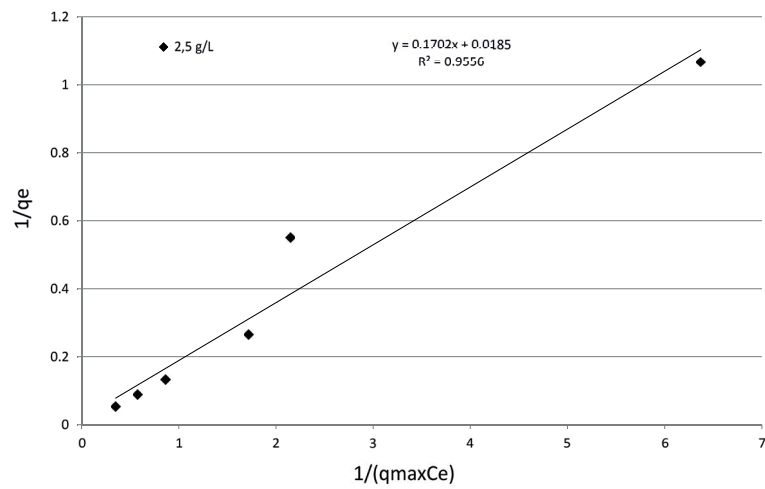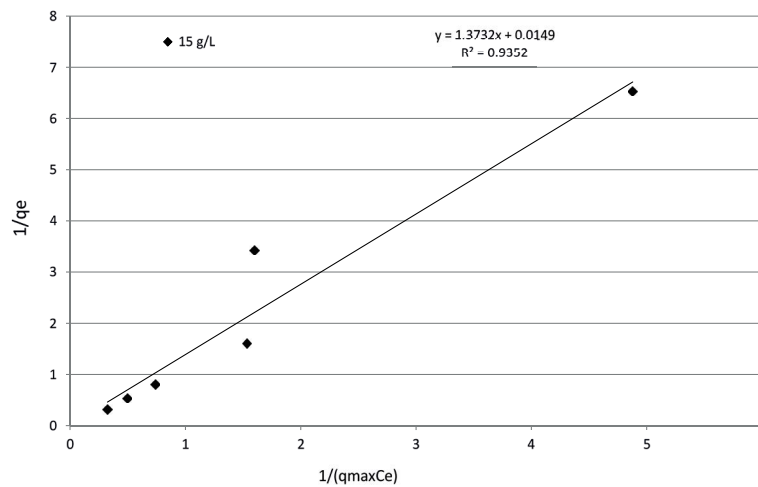

Fig. S11. Langmuir kinetic isotherm for the biosorption of Cu(II) with brewer's spent grains (particle-size range < 0.212 mm, biosorbent dosage 2.5 g/L, initial pH 4, initial concentration of Cu(II) 2.5–50 mg/L).
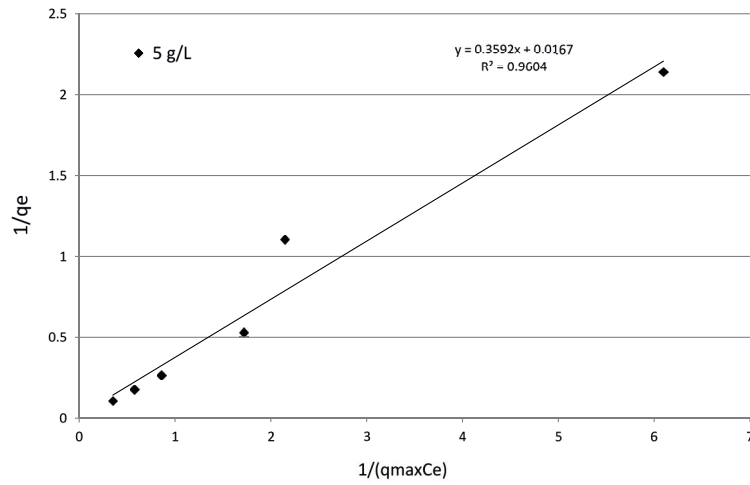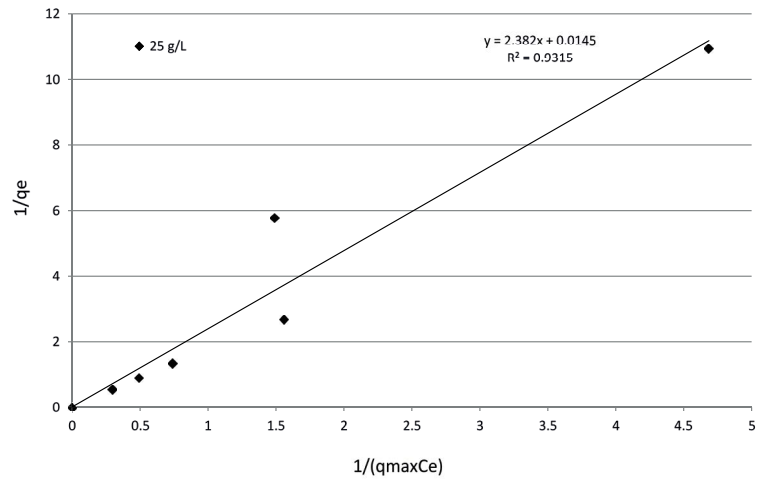
Fig. S12. Langmuir kinetic isotherm for the biosorption of Cu(II) with brewer's spent grains (particle-size range < 0.212 mm, biosorbent dosage 5 g/L, initial pH 4, initial concentration of Cu(II) 2.5–50 mg/L).
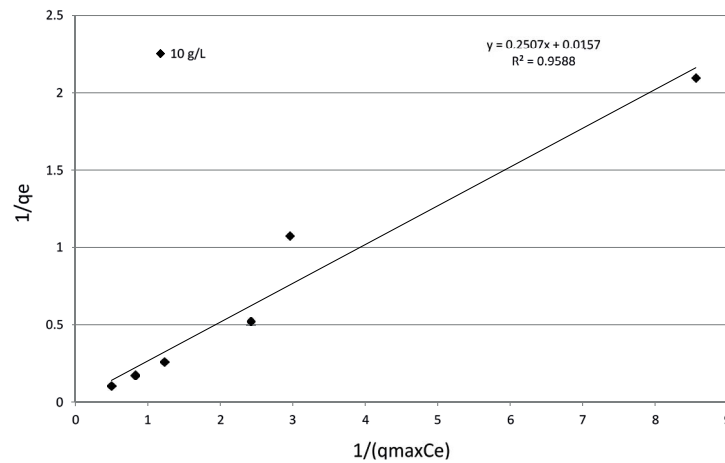
Fig. S13. Langmuir kinetic isotherm for the biosorption of Cu(II) with brewer's spent grains (particle-size range < 0.212 mm, biosorbent dosage 10 g/L, initial pH 4, initial concentration of Cu(II) 2.5–50 mg/L).

Fig. S14. Langmuir kinetic isotherm for the biosorption of Cu(II) with brewer's spent grains (particle-size range < 0.212 mm, biosorbent dosage 15 g/L, initial pH 4, initial concentration of Cu(II) 2.5–50 mg/L).

Fig. S15. Langmuir kinetic isotherm for the biosorption of Cu(II) with brewer's spent grains (particle-size range < 0.212 mm, biosorbent dosage 25 g/L, initial pH 4, initial concentration of Cu(II) 2.5–50 mg/L).
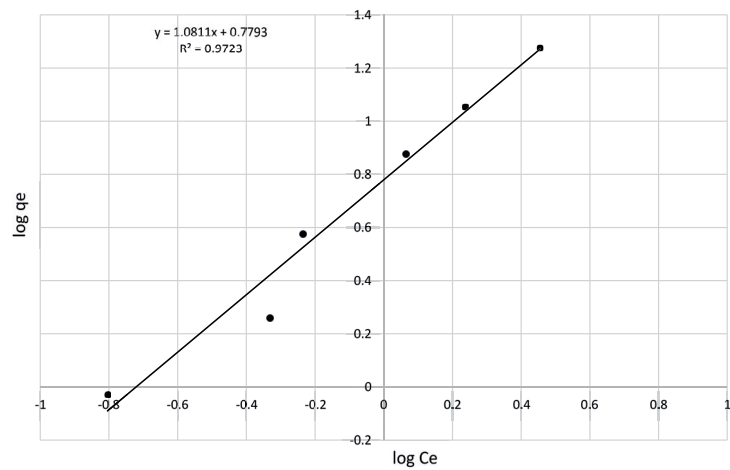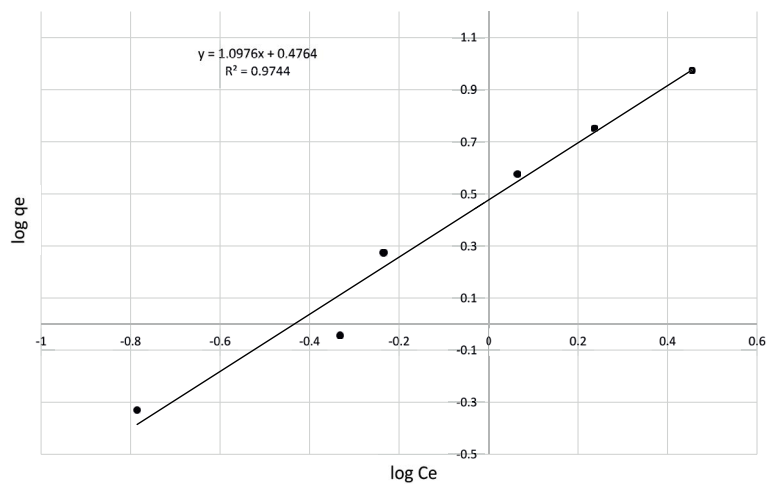

Fig. S16. Freundlich kinetic isotherm for the biosorption of Cu(II) with brewer's spent grains (particle-size range < 0.212 mm, biosorbent dosage 2.5 g/L, initial pH 4, initial concentration of Cu(II) 2.5–50 mg/L).
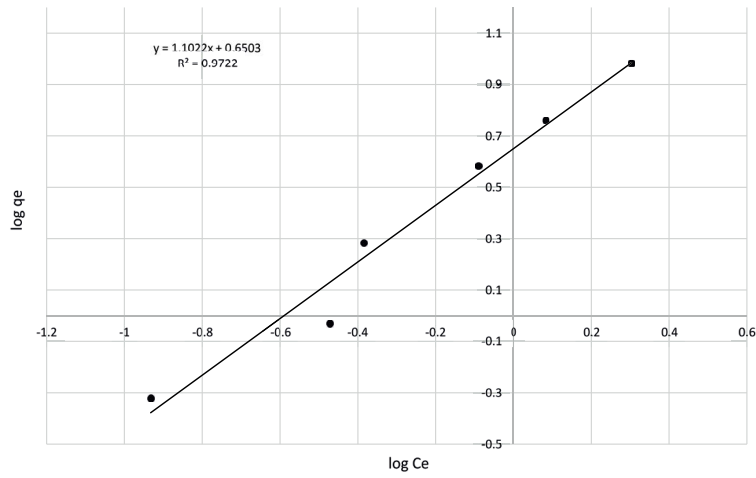

Fig. S17. Freundlich kinetic isotherm for the biosorption of Cu(II) with brewer's spent grains (particle-size range < 0.212 mm, biosorbent dosage 5 g/L, initial pH 4, initial concentration of Cu(II) 2.5–50 mg/L).

Fig. S18. Freundlich kinetic isotherm for the biosorption of Cu(II) with brewer's spent grains (particle-size range < 0.212 mm, biosorbent dosage 10 g/L, initial pH 4, initial concentration of Cu(II) 2.5–50 mg/L).
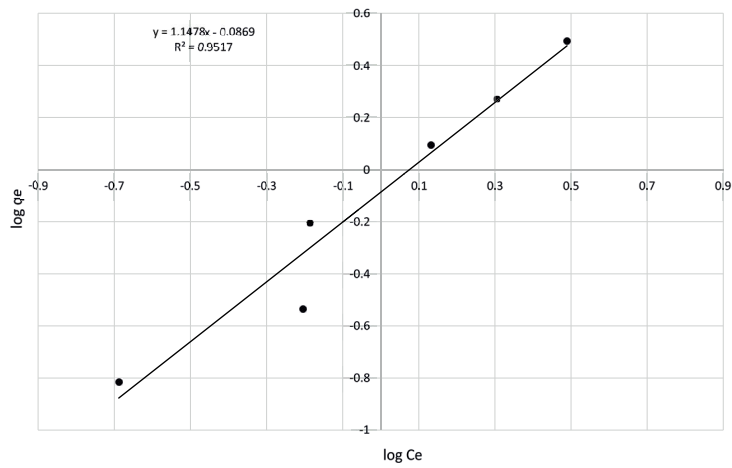

Fig. S19. Freundlich kinetic isotherm for the biosorption of Cu(II) with brewer's spent grains (particle-size range < 0.212 mm, biosorbent dosage 15 g/L, initial pH 4, initial concentration of Cu(II) 2.5–50 mg/L).
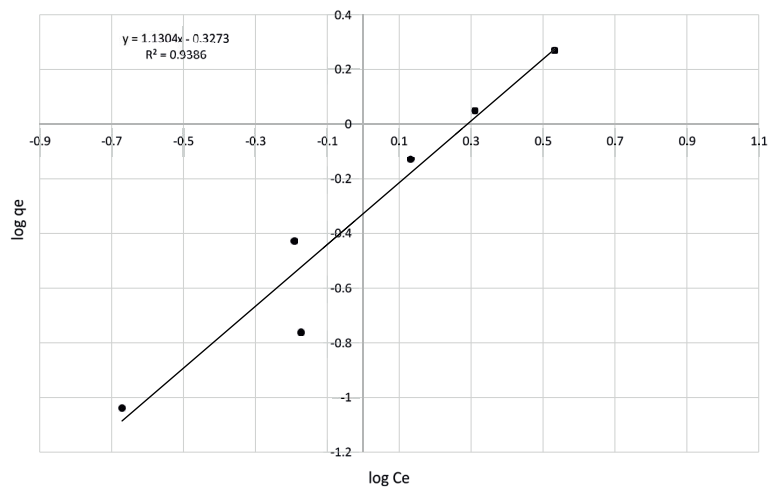

Fig. S20. Freundlich kinetic isotherm for the biosorption of Cu(II) with brewer's spent grains (particle-size range < 0.212 mm, biosorbent dosage 25 g/L, initial pH 4, initial concentration of Cu(II) 2.5–50 mg/L).

(6) Thermal stability was determined by thermogravimetric analysis using the apparatus Setsup DTG, DTA 1200 (Setram). Fly ash samples were heated at the speed 10°C/min. in the temperature range 30°C–1,000°C under nitrogen atmosphere at a flow rate of 20 mL/min.

(7) The morphology of the fly ash samples was examined with a SEM EVO-40 (Carl Zeiss, Germany).

(8) The surface structure of fly ash was examined in infrared spectroscopy using a Fourier-transform infrared-attenuated total reflection (FT-IR ATR) Spectrum 100 (Perkin-Elmer, Waltham, USA).